BES Analysis Memo
May 5, 1998
revised June 8, 1998
revised August 27, 1998

Isospin violations in $\psi(2S) \rightarrow$ vector- plus pseudoscalar-meson decays

Stephen L. Olsen
University of Hawaii

-ABSTRACT-

I report studies of isospin violations in $\psi(2S) \rightarrow$ vector- plus pseudoscalar-meson decays. I observe a signal for the isospin-violating process $\psi(2S) \rightarrow \omega\pi^0$ with a branching fraction

$$\mathcal{B}(\psi_{2S} \rightarrow \omega\pi^0) = 4.2 \pm 1.8 \pm 0.6 \times 10^{-5}.$$

This is larger than the BES group's upper limit on the branching fraction of its isospin-conserving, $SU(3)$-allowed counterpart $\psi(2S) \rightarrow \rho\pi$. In addition, I see a large, isospin-violating difference between the branching fractions for the charged and neutral $\psi(2S) \rightarrow K^*\overline{K}$ decay modes:

$$\mathcal{B}(\psi_{2S} \rightarrow K^{*0}\overline{K^0} \ + \ cc) = (13.0 \pm 5.0 \pm 1.6) \times 10^{-5},$$

$$\mathcal{B}(\psi_{2S} \rightarrow K^{*+}K^- \ + \ cc) < 5.2 \times 10^{-5} \quad (90\%\mathrm{CL}).$$

The $\omega\pi^0$ measurement confirm Ye's result; the $K^*\overline{K}$ result confirms an effect first reported by Chen and Yuan. Measurements of the R ratios for $e^+e^- \rightarrow \omega\pi^0$ and $K^*\overline{K}$ at $E_{cm} = 4.03$ GeV are presented for the first time. These results indicate that the observed isospin violations may not be solely attributable to the single photon annihilation process.

1 Introduction

The strong suppression of $\psi(2S) \rightarrow \rho\pi$ and $K^*\overline{K}$ decays is well known and has been a subject for considerable experimental [1, 2] and theoretical [3, 4, 5, 6, 7, 8] activity. No evidence is seen for $\psi(2S) \to \rho\pi$ decays in the BES group's 3.8M $\psi(2S)$ event sample [2], in striking contrast to the case for the J/ψ, where $J/\psi \to \rho\pi$ is a significant decay ($\sim$1%) [9]. This conundrum, sometimes referred to as the "$\rho\pi$ puzzle," remains one of the most intriguing mysteries in quarkonium physics.

It is expected that the dominant hadronic decay mechanism for the J/ψ and $\psi(2S)$ is the annihilation of the constituent $c\bar{c}$ quarks into three gluons (ggg). In this case, the width for the process is proportional to $\alpha_s^3(M_\psi)|\Psi(0)|^2$, where $\alpha_s(M)$ is the value of the strong coupling strength at the mass of the meson state and $\Psi(0)$ is the value of the $c\bar{c}$ wave function at zero separation distance [10]. Since the width for purely leptonic decays (e.g. $\psi(nS) \to \mu^+\mu^-$) is also proportional to $|\Psi(0)|^2$, we have the relation

$$\frac{\mathcal{B}(\psi(2S) \to \text{hadrons})}{\mathcal{B}(J/\psi \to \text{hadrons})} = \frac{\alpha_s^3(M_{\psi_{2S}})}{\alpha_s^3(M_{J/\psi})} \frac{\mathcal{B}(\psi(2S) \to \mu^+\mu^-)}{\mathcal{B}(J/\psi \to \mu^+\mu^-)} = 0.122 \pm 0.019, \quad (1)$$

where I have taken values for α_s and the lepton-pair branching fractions from the Particle Data Group (PDG) tables [9]. Although this relation is only valid for the total hadronic widths, it has been used as a standard of comparison for specific hadronic decay channels. The BES group's recently reported 90% confidence level (CL) upper limit of $\mathcal{B}(\psi(2S) \to \rho\pi) < 2.6 \times 10^5$ [2] implies

$$\frac{\mathcal{B}(\psi(2S) \to \rho\pi)}{\mathcal{B}(J/\psi \to \rho\pi)} < 2.0 \times 10^{-3}, \quad (2)$$

which is a factor of $\sim$60 below the naive expectation of Eq. 1.

The BES group has reported two interesting new results that may provide important clues that ultimately lead to an explanation of the $\rho\pi$ puzzle: Ye Shuwei has reported no apparent suppression for the isospin-violating decay $\psi(2S) \to \omega\pi^0$ [11], and Chen Yu and Yuan Changzheng have observed a large discrepancy between the $\psi(2S) \to K^{*0}\overline{K^0}$ and $K^{*+}K^-$ decay rates [12], which violates expectations from isospin conservation.

Isospin violations arise from quark-mass differences and electromagnetic (EM) processes. The lowest-order EM diagrams are the single-photon (γ^*) and the γgg processes shown in Figs. 1a and b. If the γ^* process dominates, similar isospin-violating effects should be visible in continuum e^+e^- annihilation.

In the case where the γ^* process dominates, both $\psi \to \omega\pi$ decays (here I use ψ to denote the J/ψ and $\psi(2S)$ charmonium states) and the continuum $e^+e^- \to \omega\pi$ production can be related to a form factor $f(q^2)$, whose value at $q^2 = 0$ is well determined from the $\omega \to \gamma\pi^0$ decay width. For charmonium decays, the ratio of the

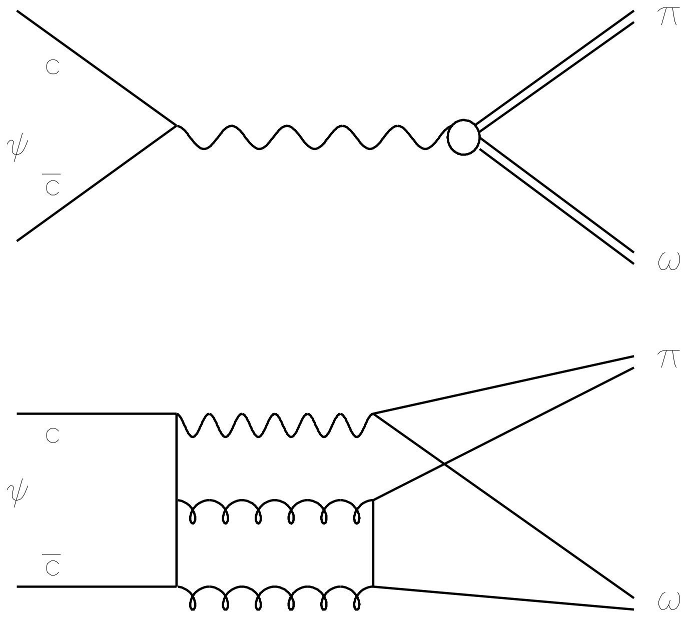

Figure 1: The lowest order diagrams for $\psi \to \omega\pi^0$.

electromagnetic factors at $q^2 = m_\psi^2$ and at $q^2 = 0$ is given in ref. citecoffman

$$\frac{|f(m_\psi^2)|^2}{|f(0)|^2} = \frac{\alpha}{3}\left[\frac{p_\gamma}{p_\omega}\right]^3 \frac{m_\psi}{\Gamma(\omega \to \gamma\pi^0)} \frac{\Gamma(\psi \to \omega\pi^0)}{\Gamma(\psi \to \mu^+\mu^-)} \tag{3}$$

This relation is readily extended to the continuum $e^+e^- \to \omega\pi^0$ process

$$\frac{|f(s)|^2}{|f(0)|^2} = \frac{\alpha}{3}\left[\frac{p_\gamma}{p_\omega}\right]^3 \frac{\sqrt{s}}{\Gamma(\omega \to \gamma\pi^0)} R_{\omega\pi}(s) \tag{4}$$

where $R_{\omega\pi}$ is the ratio of the Born-level cross section for $e^+e^- \to \omega\pi$ to the lowest level QED cross section for $e^+e^- \to \mu^+\mu^-$. These relations are independent of the explicit form of $f(q^2)$. In the vector dominance model (VDM), the form factor is mediated by one or more vector mesons V^*, as indicated in Fig. 2. In this case, the form factor has the functional form

$$f(q^2) \sim \frac{f(0)}{1 - q^2/m^{*2}}, \tag{5}$$

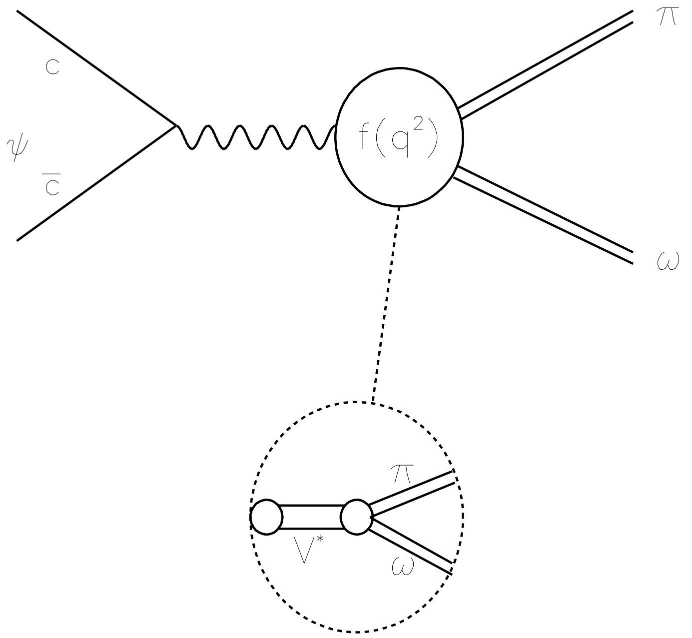

Figure 2: The single-photon annihilation diagram for $\omega\pi^0$ production. The bubble indicates the VMD picture for the form factor at the $\gamma\omega\pi$ vetex.

where m^* is some effective mass of the vector mesons involved.

In the following, I describe independent attempts to reproduce the BES results on $\omega\pi^0$ and $K^*\overline{K}$, and report first measurements of $R_{\omega\pi}$ and $R_{K^*\overline{K}}$ using the 4.03 GeV data. In the discussion, I examine the $\omega\pi$ results in the context of the $\gamma\omega\pi$ form factor discussed above.

2 Event preselection

For the analyses reported here, I use the $\psi(2S)$ event samples on the two- and four-prong data summary tapes and all of the 4.03 GeV data. I only use charged tracks and gammas that are in the $|\cos\theta| < 0.8$ polar angle region. I veto events where the highest momentum positive *and* negative tracks are *both* identified either as muons or electrons. This eliminates most of the $\psi(2S) \to J/\psi$ cascade events where the

J/ψ decays to lepton pairs. For each final state studied, events are required to have the appropriate number of tracks with zero net charge. Gammas are associated with neutral clusters in the BSC with energies greater than 50 MeV. In the event that the number of neutral clusters exceeds the minimum number needed for a given hypothesis, the best combination is selected by means of a four-constraint kinematic fit. In the following tables, these criteria are included in the category labeled "preselection."

For the number of $\psi(2S)$ events in the data sample, I use the number $N_{\psi_{2S}} = (3.44 \pm 0.31) \times 10^6$ that was determined from the number of $\psi(2S) \to \pi^+\pi^- J/\psi$; $J/\psi \to \mu^+\mu^-$ events found on the four-prong data summary tapes [14]. This number is determined using similar charged-track requirements as is used in the analysis reported here, which will tend to cancel errors associated with extra "ghost" tracks, etc.

3 $\psi(2S) \to \omega\pi^0$

For $\psi(2S) \to \omega\pi^0$, the reaction of interest is $\psi(2S) \to \pi^+\pi^-\pi^0\pi^0 \to \pi^+\pi^- 4\gamma$. I select events with two oppositely charged tracks and four or more candidate gammas. For events with more than four candidate gammas, I select the four gamma combination that produces the best χ^2 value from a 4-c kinematic fit to the hypothesis $\psi(2S) \to \pi^+\pi^- 4\gamma$. Since the charged $\pi^+\pi^-$ pair must come from the decay $\omega \to \pi^+\pi^-\pi^0$, I require $M_{\pi^+\pi^-} < 0.62$ GeV. Cascade $\psi(2S) \to \pi^+\pi^- J/\psi$ events are removed by eliminating events where the mass recoiling against the $\pi^+\pi^-$ pair is within 50 MeV of the J/ψ.

I used 1000 simulated $\psi(2S) \to \omega\pi^0$ events generated by the HOWL Monte Carlo simulator to develop the final selection criteria: $|M_{\gamma_i\gamma_j} - M_{\pi^0}| < 0.035$ GeV. Distributions of the various cut variables are presented for the MC data in Figs. 3a through f. Figure 3f shows the $M_{\pi^+\pi^-\pi^0}$ distribution recoiling against a π^0. A total of 76 simulated events survive the selection procedure, indicating an acceptance of $\varepsilon_{\omega\pi} = 0.08 \pm 0.01$.

Figures 4a through 4f show the results of the application of the selection criteria to the $\psi(2S)$ data. Figure 4e shows the invariant mass distribution for $\pi^+\pi^-\pi^0$ combinations recoiling against a $\gamma\gamma$ pair with invariant mass within 35 MeV of M_{π^0}. A peak is evident at M_ω. A fit to this distribution using a Gaussian-smeared Breit-Wigner signal function with mass and width fixed at $M_\omega = 0.782$ GeV and $\Gamma_\omega = 0.008$ GeV, and smeared by the MC-determined mass resolution of $\sigma = 0.018$ GeV plus a smooth background yields the number of signal events $N^{evt}_{\omega\pi^0} = 9.8 \pm 4.3$. Figure 4d shows the $\gamma\gamma$ mass distribution recoiling against $\pi^+\pi^-\pi^0$ combinations with invariant masses within 50 MeV of M_ω, where a π^0 peak is apparent. A fit to this distribution using a

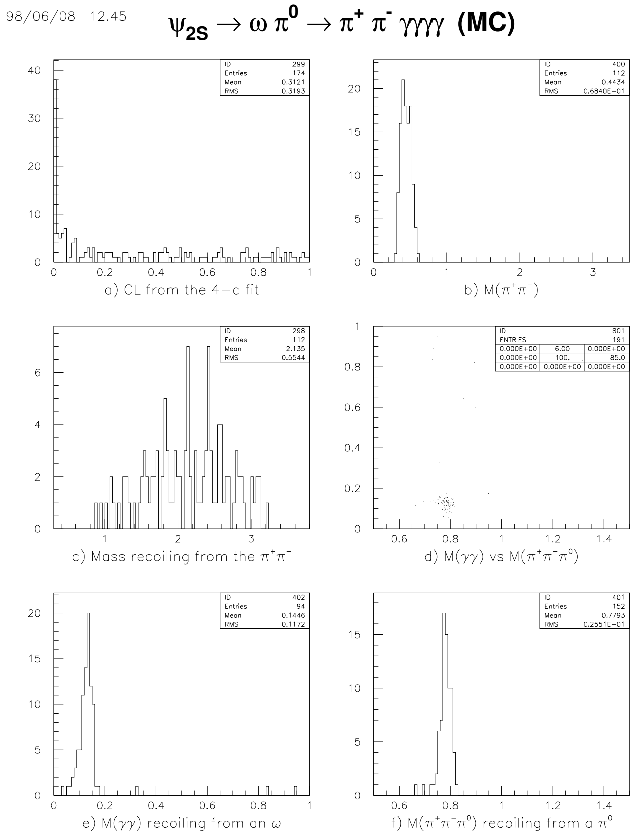

Figure 3: Distributions for MC simulated $\psi(2S) \to \omega\pi^0$ events: **a)** the confidence level from the 4-c kinematic fit; **b)** $M_{\pi^+\pi^-}$; **c)** the mass recoiling against the $\pi^+\pi^-$ pair; **d)** $M_{\gamma\gamma}$ (y) versus $M_{\pi^+\pi^-\pi^0}$ (x); **e)** $M_{\gamma\gamma}$ recoiling against a $\pi^+\pi^-\pi^0$ combination with an invariant mass within 50 MeV of M_ω; **f)** $M_{\pi^+\pi^-\pi^0}$ recoiling against a π^0.

smooth background and a Gaussian with $\sigma = 18$ MeV yields 8.5 ± 4.0 π^0s, in reasonable agreement with the fit to the ω peak. A summary of the cuts and the number of events that survive them is presented in Table 1.

I determine the $\psi(2S) \to \omega\pi^0$ branching fraction from the relation

$$\mathcal{B}(\psi_{2S} \to \omega\pi^0) = \frac{N^{evt}_{\omega\pi^0}}{N_{\psi_{2S}}\mathcal{B}(\omega \to \pi^+\pi^-\pi^0)\mathcal{B}(\pi^0 \to \gamma\gamma)^2\varepsilon_{\omega\pi}} = (4.2 \pm 1.8 \pm 0.6) \times 10^{-5}, \quad (6)$$

which is in good agreement with Ye's result of $(3.8 \pm 1.7 \pm 1.1) \times 10^{-5}$ [11].

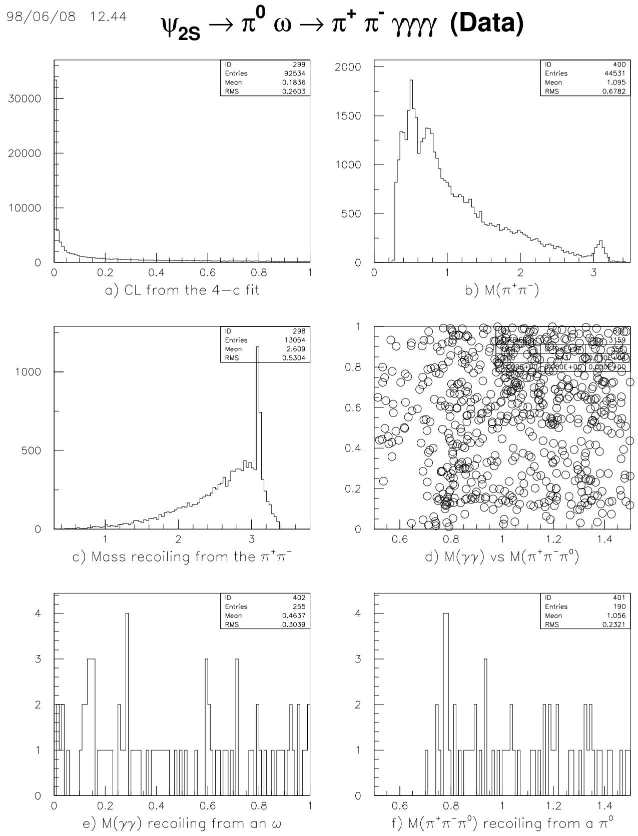

Figure 4: The distributions of Fig. 3 for $\psi(2S) \to \pi^+\pi^-4\gamma$ events.

4 $\psi(2S) \to K^*\overline{K}$

For the $\psi(2S) \to K^*\overline{K}$ measurement I investigate the decay chains

$$\psi(2S) \to \overline{K^{*0}}\, K^0 \quad (K^0 \to \pi^+\pi^-,\ \overline{K^{*0}} \to K^-\pi^+) \qquad , \qquad \psi(2S) \to K^{*+} K^- \quad (K^{*+} \to K^0\pi^+,\ K^0 \to \pi^+\pi^-)$$

and their charged conjugates. For these reactions, both channels have the same $K^\pm\pi^\mp K^0$; $K^0 \to \pi^+\pi^-$ final state and I use the same selection and event sample for the two channels.

I subjected events with four charged tracks and zero net charge to a 4-c fit to the to the hypothesis $\psi(2S) \to K^+\pi^-\pi^+\pi^-$ and a 5-c fit where the additional constraint is that one $\pi^+\pi^-$ pair is consistent with $K^0 \to \pi^+\pi^-$. I selected events that pass the 5-c

Table 1: A tabulation of the $\psi(2S) \to \omega\pi^0$ selection cuts.

The number of events surviving each requirement

	data	Monte Carlo
Generated		1000
Preselection	215370	192
$CL_{4c} > 0.05$	44531	112
$M_{\pi^+\pi^-} < 0.62$ GeV	13054	112
$\lvert MM_{\pi^+\pi^-} - M_{J/\psi}\rvert > 0.05$ GeV	10831	108
$\lvert M_{\gamma_i\gamma_j} - M_{\pi^0}\rvert < 0.035$ GeV		
$\lvert M_{\gamma_k\gamma_l} - M_{\pi^0}\rvert < 0.035$ GeV	95	76
$M_{\pi^+\pi^-\pi^0} = M_\omega$	9.8	76

fit with a CL greater than 5%. To eliminate the numerous $\psi(2S) \to \pi^+\pi^- J/\psi;\ \ J/\psi \to \ell^+\ell^-$ cascade events, I reject events where the mass recoiling against any $\pi^+\pi^-$ pair is within 50 MeV of $M_{J/\psi}$.

Figure 5 shows, on a semilog scale, the $c\tau$ distribution for the candidate $K^0 \to \pi^+\pi^-$ pairs that survive the selections described above. Superimposed on the data is the results of a fit including a Gaussian to represent the prompt, non-K^0 background and an exponential with $c\tau = 0.0267$ m to represent a K^0 signal. The fit indicates that there is a K^0 signal corresponding to 81 ± 12 events. I eliminate the prompt, non-K^0 backgrounds by requiring that the $K^0 \to \pi^+\pi^-$ vertex is displaced from the interaction point by a proper length greater that $c\tau = 0.0126$ m. The number of events satisfying the various cuts are summarized below in Table 2. The effects of the cuts on 1000 simulated $\psi(2S) \to K^{*0}\overline{K^0} \to K^+\pi^-\pi^+\pi^-$ events are also indicated in the table.

Figures 6a and b show the $K^\pm\pi^\mp$ and $K^0\pi^\pm$ invariant mass distributions, respectively, for the events that satisfy the selection criteria. While there is a prominent peak in the $K^\pm\pi^\mp$ mass distribution at the position of $K^{*0}(895)$, there is no evidence for a corresponding signal in the $K^0\pi^\pm$ channel.

In Fig. 7, I show the $K^\pm\pi^\mp$ mass distribution together with the results of a fit using a P-wave Breit Wigner function convoluted with a Gaussian resolution function with $\sigma = 0.015$ GeV to represent the K^{*0}, and a smooth background function that is constrained to be zero for masses below the $K\pi$ threshold. The fit gives a total of 15.0 ± 6.3 K^{*0} events. The $K^0\pi^\pm$ mass distribution has only two events within $\pm\Gamma$ of

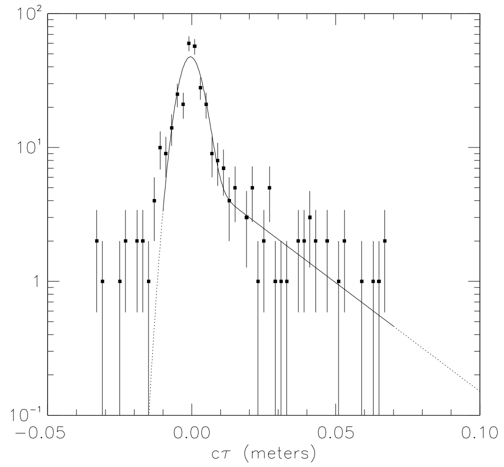

Figure 5: The $c\tau$ distribution for the candidate $K^0 \to \pi^+\pi^-$ pairs.

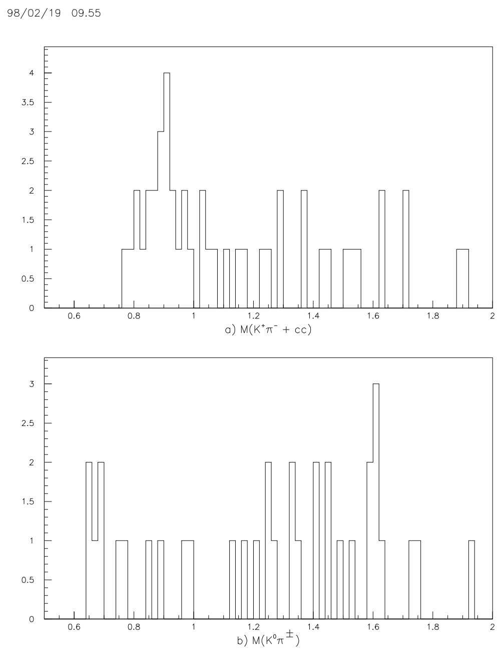

Figure 6: The invariant **a)** $K^\pm\pi^\mp$ and **b)** $K^0\pi^\pm$ mass distributions for the events that satisfy all of the selection criteria.

Table 2: A tabulation of the $\psi(2S) \to K^*\overline{K}$ selection cuts.

The number of events surviving each requirement

	data	Monte Carlo
Generated		1000
Preselection ($N_{chg} = 4;\ \Sigma Q = 0$)	921027	661
$CL_{5c} > 0.02$	1354	349
$\lvert MM_{\pi^+\pi^-} - M_{J/\psi}\rvert > 0.05$ GeV	335	348
$c\tau > 0.0126$ m	50	192

M_{K^*}, which are consistent with the background level. Treating both events as real, I infer a 90% CL upper limit of 5.3 events.

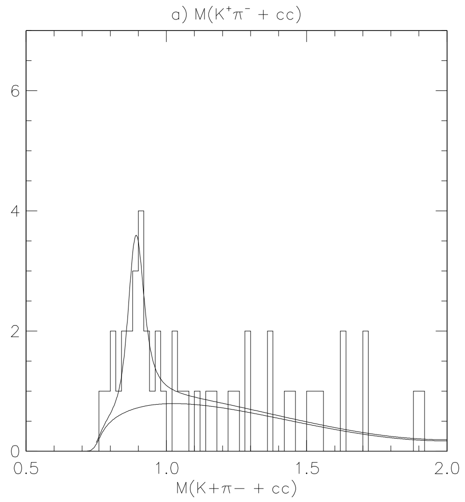

Figure 7: A fit to the $K^\pm\pi^\mp$ invariant mass distribution using a resolution-broadened Breit Wigner with the $K^{*0}(896)$ mass and width and a smooth background function.

I determine the $\psi(2S) \to K^{*0}\overline{K^0}$ branching fraction from the relation

$$\mathcal{B}(\psi_{2S} \to K^{*0}\overline{K^0}) = \frac{N^{evt}_{K^{*0}\overline{K^0}}}{N_{\psi_{2S}}\mathcal{B}(K^{*0} \to K^+\pi^-)(\mathcal{B}(\overline{K^0} \to \pi^+\pi^-)\varepsilon_{K^*K}}, \tag{7}$$

where $\varepsilon_{K^*K} = 0.146 \pm 0.012$ is the MC-determined acceptance. I use $\mathcal{B}(\overline{K^0} \to \pi^+\pi^-) = 0.343 \pm 0.001$, which includes a factor of 0.5 to account for the probability that the $\overline{K^0}$ becomes a K_s, and $\mathcal{B}(K^{*0} \to K^+\pi^-) = 2/3$ [15]. The result is

$$\mathcal{B}(\psi_{2S} \to K^{*0}\overline{K^0} \ + \ cc) = (13.0 \pm 5.0 \pm 1.6) \times 10^{-5}, \tag{8}$$

which is higher than, but not inconsistent with, the IHEP result of $(8.1 \pm 2.4 \pm 1.6) \times 10^{-5}$ [12].

For the $\psi(2S) \to K^{*+}K^-$ branching fraction, I use the 5.3 event upper limit and the MC-determined acceptance for this channel of 0.130 ± 0.012 to etablish the limit

$$\mathcal{B}(\psi_{2S} \to K^{*+}K^- \ + \ cc) < 5.2 \times 10^{-5} \quad (90\% \text{ CL}). \tag{9}$$

The large discrepancy between the $K^{*0}\overline{K^0}$ and $K^{*+}K^-$ branching fractions is contrary to expectations from isospin invariance, which would have them equal.

In the PDG listing for $J/\psi \to K^*\overline{K}$ decays, the $K^{*0}\overline{K^0}$ branching fraction is about 20% lower than that for $K^{*+}K^-$ [9]:

$$\frac{\mathcal{B}(J/\psi \to K^{*0}\overline{K^0})}{\mathcal{B}(J/\psi \to K^{*+}K^-)} = \frac{(4.2 \pm 0.4) \times 10^{-3}}{(5.0 \pm 0.4) \times 10^{-3}} = 0.84 \pm 0.12, \tag{10}$$

an effect that has been attributed to u- and d-quark mass differences [13]. Our results for the $\psi(2S)$ are opposite; we find the $K^{*0}\overline{K^0}$ branching fraction to be larger [16]:

$$\frac{\mathcal{B}(\psi_{2S} \to K^{*0}\overline{K^0})}{\mathcal{B}(\psi_{2S} \to K^{*+}K^-)} > 1.5 \quad (90\% \text{ CL}). \tag{11}$$

5 $e^+e^- \to \omega\pi$ and $K^*\overline{K}$ at $\sqrt{s} = 4.03$ GeV

I applied the $\omega\pi$ and $K^*\overline{K}$ selection criteria described above to the 22.3 $pb{-}1$ data sample at $\sqrt{s} = 4.03$ GeV.

5.1 $e^+e^- \to \omega\pi^0$

Figure 8 shows the precut distributions for the same kinematic variables shown in Figs. 3 and 4. In Fig. 8d, which is a scatterplot of $M_{\gamma\gamma}$ (vertical) versus $M_{\pi^+\pi^-\pi^0}$ (horizontal) shows a small cluster of events corresponding to $\omega\pi^0$ production. Figure 8e shows the invariant mass distribution for $\gamma\gamma$ pairs recoiling against $\pi^+\pi^-\pi^0$ combinations with invariant mass within ± 50 MeV of M_ω; Fig. 8f shows the invariant mass distribution for $\pi^+\pi^-\pi^0$ combinations recoiling against $\gamma\gamma$ pairs that have a mass within $\pm$ 35 MeV of M_{π^0}. Fitting the $\pi^+\pi^-\pi^0$ mass distribution of Fig. 8f with with a resolution-broadened Breit-Wigner function plus a smooth background gives 4.5 ± 3.0 ω events; fitting the $\gamma\gamma$ mass distribution of Fig. 8e with a Gaussian with a peak value at M_{π^0} and width fixed at the MC-determined mass resolution of $\sigma = 18$ MeV and a smooth background gives 5.3 ± 2.8 π^0 events. I use the average of these two numbers, namely 4.9 ± 2.9 as the number of $\omega\pi^0$ events.

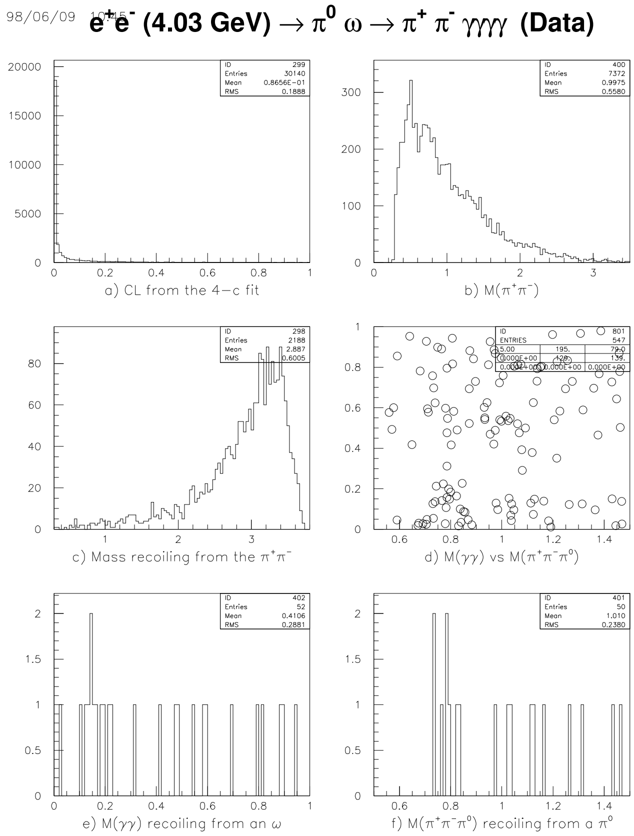

Figure 8: The distributions of Fig. 3 for $e^+e^- \to \pi^+\pi^-4\gamma$ events at $\sqrt{s} = 4.03$ GeV.

5.2 $e^+e^- \to K^*\overline{K}$

Figures 9a and b show the invariant $K^\pm\pi^\mp$ and $K^0\pi^\pm$ mass distributions, respectively, for events that satisfy all of the selection criteria for $e^+e^- \to K^\pm\pi^\mp K^0$ at $\sqrt{s} =$ 4.03 GeV. There are some $K^\pm\pi^\mp$ events with mass in the $K^*(890)$ region; the $K^0\pi^\pm$ distribution has none. A fit to the $K^\pm\pi^\mp$ mass distribution (Fig. 9a) yields 7.4 ± 3.6

K^{*0} events. From the zero $K^{*\pm} \to K^0\pi^p m$ events, I infer a 90% CL upper limit of 2.3 events.

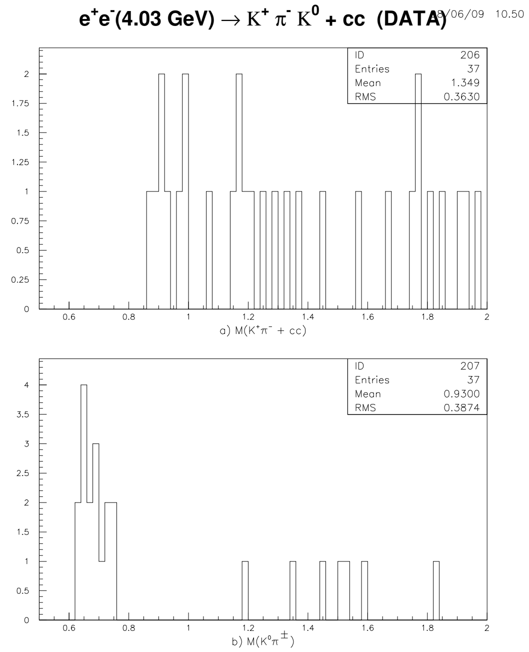

Figure 9: The invariant **a)** $K^{\pm}\pi^{\mp}$ and **b)** $K^0\pi^{\pm}$ mass distributions for the events that satisfy all of the selection criteria for $e^+e^- \to K^{\pm}\pi^{\mp}K^0$ at $\sqrt{s} = 4.03$ GeV.

5.3 Determination of $R_{\omega\pi}$ and R_{K^*K}

I determine the R values from the number of events from the relation

$$R = \frac{N_{evts}}{\mathcal{L}(1+\delta)\varepsilon\mathcal{B}\sigma_{QED}(e^+e^- \to \mu^+\mu^-)}, \tag{12}$$

where $\mathcal{L} = 22.3$ pb^{-1} is the integrated luminosity, $\mathcal{B}$ denotes the various branching fractions (listed explicitly in Eqns. 6 and 7), $\sigma_{QED}(e^+e^- \to \mu^+\mu^-) = 5.34$ nb, ε is the acceptance and $1+\delta$ is the radiative correction.

5.3.1 Radiative correction and acceptance

Although we are interested in determining the cross section for the Born-level process indicated in Fig. 2, the data sample can contain events from higher-order processes, most notably that involving initital state radiation (ISR) as shown in Fig. 10. Here one of the incoming beam particles radiates a photon that carries off a fraction k of its energy and the subsequent e^+e^- annihilation process occurs at a cm energy $\sqrt{s_{eff}}$ that is reduced from its nominal value $\sqrt{s_{nom}}$ by the factor $s_{eff} = (1-k)s_{nom}$.

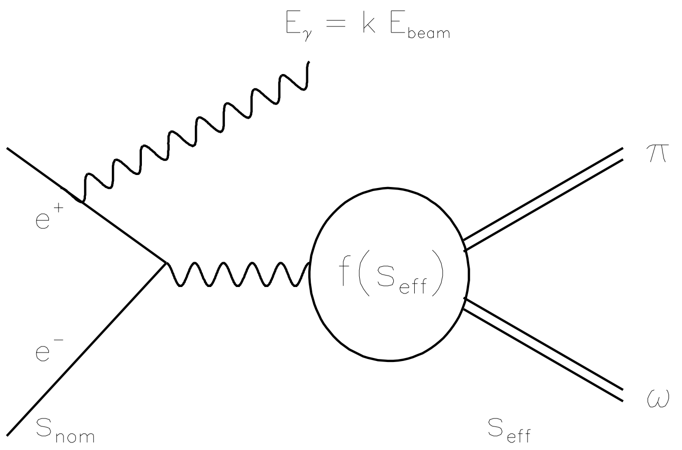

Figure 10: The initial-state-radiation diagram for $\psi \to \omega\pi^0$.

According to the formulation of Bonneau and Martin [17], $\sigma_{obs}(s_{nom})$, the observed cross section at s_{nom}, is related to $\tilde{\sigma}_B(s_{eff})$, the Born-level cross section at the reduced energy by

$$\sigma_{obs}(s_{nom}) = \int_0^1 dk \cdot f(k, s_{nom})\ \tilde{\sigma}_B(s_{eff}). \tag{13}$$

Here $f(k, s_{nom})$ is the sampling function that represents the effective luminosity at s_{nom} and is given by

$$f(k, s_{nom}) = \beta \left[k^{\beta-1}(1+\delta_1) + k/2 \right] - \beta, \tag{14}$$

where

$$\beta = \frac{2\alpha}{\pi} \left[\ln\left(\frac{s_{nom}}{m_e^2}\right) + 1 \right] = 0.07876 \tag{15}$$

and

$$\delta = \frac{3\beta}{4} + \frac{\alpha}{\pi}\left[\frac{\pi^2}{3} + \frac{1}{2}\right] = 0.06555 \tag{16}$$

In order to apply this formalism, some model for the energy dependence of $\tilde{\sigma}_B$ must be invoked. I use the parameterization:

$$\tilde{\sigma}_B(s_{eff}) = \tilde{\sigma}_B(s_{nom})\left(\frac{s_{nom}}{s_{eff}}\right)^n, \tag{17}$$

where $n = 3$ corresponds to the high energy behaviour of the VMD model for the $\gamma\omega\pi$ form factor. With this parameterization, the radiative correction is:

$$1 + \delta \equiv \frac{\sigma_{obs}(s_{nom})}{\tilde{\sigma}_B(s_{nom})} = \int_0^1 dk \cdot f(k, s_{nom})\left(\frac{s_{nom}}{s_{eff}}\right)^n \tag{18}$$

I calculate the radiative correction by evaluating the integral in Eq. 18 numerically for values of n ranging from 1 to 4. For each case, I compute the experimental acceptance by generating MC events with ISR included. The results are listed in Table 3. Events that have an ISR photon with substantial energy do not satisfy the selection criteria and models with larger radiative corrections have smaller acceptances. Thus, although in going from $n = 2$ to $n = 3$, the radiative correction increases by a factor of 1.7, the product of the radiative correction and the acceptance changes by less than 30%. For $n \geq 4$ the radiative correction gets very large and the present calculation is probably not applicable. For determining the R values, I use the $n = 3$ result for $(1+\delta)\varepsilon$ and assign the difference between the $n = 2$ and $n = 3$ values as the estimated error. If, in fact, $n \geq 4$ is a better model for $\tilde{\sigma}_B$, the results here can be considered as an upper limit on the R values.

5.4 Results for $R_{\omega\pi}$, $R_{K^{*0}K}$ and $R_{K^{*+}K^-}$

The resulting values for $R_{\omega\pi}$ and $R_{K^{*0}K}$, and the 90% CL upper limit for $R_{K^{*+}K^-}$ are:

$$\begin{aligned} R_{\omega\pi} &= (0.53 \pm 0.33) \times 10^{-3}, \\ R_{K^{*0}K} &= (1.24 \pm 0.63) \times 10^{-3}, \\ R_{K^{*+}K^-} &< 0.39 \times 10^{-3}. \end{aligned} \tag{19}$$

The $R_{\omega\pi}$ value is substantially smaller than the ratio of the $\psi \to \omega\pi$ and $\psi \to \mu^+\mu^-$ decay widths:

$$\frac{\Gamma(J/\psi \to \omega\pi)}{\Gamma(J/\psi \to \mu^+\mu^-)} = (7.0 \pm 1.0) \times 10^{-3} \tag{20}$$

Table 3: Radiative corrections and acceptance for $e^+e^- \to \omega\pi^0$ at $\sqrt{s} = 4.03$ GeV.

	n=1	n=2	n=3	n=4
	pointlike		VMD	
$1+\delta$	1.10	1.49	2.57	8.24
$\varepsilon_{\omega\pi}$	0.053	0.046	0.035	0.025
$(1+\delta)\varepsilon_{\omega\pi}$	0.058	0.069	0.089	0.21
ε_{K^*K}	0.163	0.14	0.086	0.040
$(1+\delta)\varepsilon_{K^*K}$	0.18	0.19	0.22	0.33

$$\frac{\Gamma(\psi(2S) \to \omega\pi)}{\Gamma(\psi(2S) \to \mu^+\mu^-)} = (4.7 \pm 2.5) \times 10^{-3}.$$

Likewise, the $R_{K^{*0}K}$ value is smaller than the ratio of the $\psi(2S) \to K^{*0}K$ and $\psi(2S) \to \mu^+\mu^-$ decay widths:

$$\frac{\Gamma(\psi(2S) \to K^{*0}K + cc)}{\Gamma(\psi(2S) \to \mu^+\mu^-)} = (1.7 \pm 0.6) \times 10^{-2}. \tag{21}$$

The difference between $e^+e^- \to K^{*0}K$ and $e^+e^- \to K^{*+}K^-$ has the same isospin-violating character as seen in $\psi(2S)$ decays (see Eqn. 11) [16]

$$\frac{R_{K^{*0}K}}{R_{K^{*+}K^-}} > 1.6 \quad (90\%\ \mathrm{CL}). \tag{22}$$

6 Discussion

In contrast to $\psi(2S) \to \rho\pi$ decays, there does not appear to be any anomalous suppression for $\psi(2S) \to \omega\pi$ relative to J/ψ decays. The ratio

$$\frac{\mathcal{B}(\psi_{2S} \to \omega\pi)}{\mathcal{B}(J/\psi \to \omega\pi)} = 0.10 \pm 0.05 \tag{23}$$

is in reasonable agreement with the expected ratio of the total hadronic decays given above in Eqn. 1. This seems to rule out explanations for the $\rho\pi$ puzzle that depend on the spin-parity of the final-state particles [4] and those that invoke form factors [5] or wave-function overlaps [6, 7]. A recent explanation that attributes the $\rho\pi$ puzzle to the influence of a $^3S_1$ color-octet $c\bar{c}$ state predicts no suppression for the $\omega\pi$ channel [8]; in agreement with our measurement.

Table 4: Amplitudes and reduced branching fractions for the $\psi(2S) \to VP$ decays studied here.

Decay Mode	$\mathcal{M}$	$\tilde{\mathcal{B}}(\times 10^5)$
$\rho\pi$	$\sqrt{3}(g+e)$	< 0.51
$K^{*+}K^- \ + \ cc$	$\sqrt{2}[g(1-s)+e]$	< 0.95
$K^{*0}\overline{K^0} \ + \ cc$	$\sqrt{2}[g(1-s)-2e]$	2.7 ± 1.1
$\omega\pi^0$	$3e$	0.77 ± 0.35

Seiden, Sadrozinski, and Haber provide a convenient parameterization of the amplitudes for $\psi(nS) \to VP$ decays [18]. The parameterizations relevant to the decays mentioned here are given in the column labeled $\mathcal{M}$ in Table 4. Included in the table are the measured values for the reduced branching fractions $\tilde{\mathcal{B}}$, defined as $\tilde{\mathcal{B}} \equiv \mathcal{B}/p^3$, where p is the momentum of the decay particles in the $\psi(2S)$ rest frame. In the notation of ref. [18], g is the SU(3)-conserving strong amplitude, s is a correction for SU(3) violating effects and is expected to be small ($s \sim 0.2g$), and e is the electromagnetic amplitude.

Using the normalization $\tilde{\mathcal{B}} = |\mathcal{M}|^2$, we see that the $\omega\pi$ result establishes the level of the electromagnetic amplitude at $e^2 = 0.09 \pm 0.04 \times 10^{-5}$. The other results are consistent with this if $g \simeq -e$. In the ref. [18] analysis of $J/\psi \to VP$ decays, $g \simeq +10e$. For $\psi(2S)$ decays, the SU(3)-allowed strong amplitude is suppressed by an order of magnitude, to the level of the electromagnetic term.

6.1 The $\gamma\omega\pi$ form factor

Our results for $\mathcal{B}(\psi(2S) \to \omega\pi)$ and $R_{\omega\pi}(\sqrt{s} = 4.03$ GeV), and the PDG value for $\mathcal{B}(J/\psi \to \omega\pi)$ can be applied to Eqs. 3 and 4, to provide measurements of $|f(q^2)/f(0)|$ at $q^2 = M^2_{J/\psi}$, $M^2_{\psi(2S)}$ and $(4.03 \text{ GeV})^2$. The results are tabulated in Table 5 and shown in Fig. 11. The curve in Fig. 11 is the result of a fit of a κ/q^2 functional form to the three $|f(q^2)/f(0)|$ measurements. This form, which is expected for VMD models of the form factor, fails to fit the data ($\chi^2/dof = 11.3/2$), the $R_{\omega\pi}$ value at 4.03 GeV is too small.

The results indicate that to the extent that VMD adequately describes the $\gamma\omega\pi$ form factor, single-photon annihilation may not be the dominant mechanism for the observed isospin violating $\psi(2S) \to VP$ decays. This leaves the γgg process as the remaining lowest-order possibility. Since this diagram violates hadronic helicity conservation, this would indicate that this symmetry is not well respected in charmonium decays.

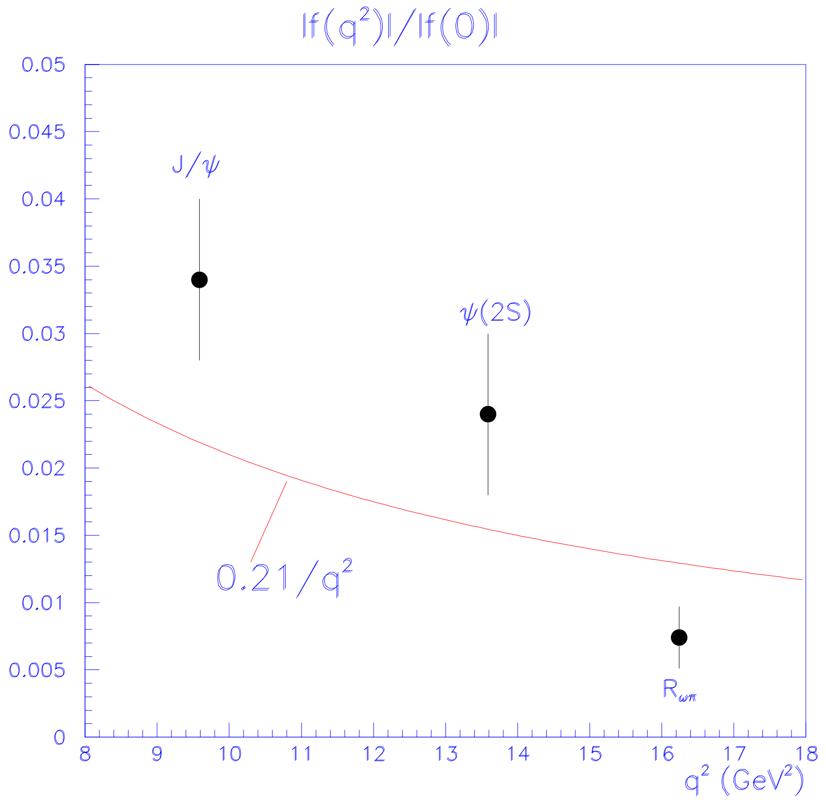

Figure 11: The $|f(q^2)/f(0)|$ values determined from the J/ψ and $\psi(2S) \to \omega\pi$ branching fractions and $R_{\omega\pi}$ at 4.03 GeV. The curve is the result of fitting the three points to the functional form κ/q^2.

7 Conclusion

We have presented evidence that the suppression seen for hadronic $\psi(2S) \to VP$ decays does not apply for isospin-violating processes. Moreover, the electromagnetic $\gamma\omega\pi$ form factor determined from $\psi(2S) \to \omega\pi$ is substantially higher than that determined from $R_{\omega\pi}$ at nearby q^2 values. This indicates that the observed isospin violations in J/ψ and $\psi(2S)$ decays may not be attributable solely to the effects of single photon annihilation. This situation could be clarified decisively by measurements of $R_{\omega\pi}$ at q^2 values near $M^2_{J/\psi}$ and $M^2_{\psi(2S)}$.

Table 5: The $\gamma\omega\pi$ form factor determined from $\mathcal{B}(\psi\omega\pi)$, $\psi = J/\psi$ and $\psi(2S)$, and $R_{\omega\pi}(4.03\text{ GeV})$.

q^2	$M^2_{J/\psi}$	$M^2_{\psi(2S)}$	$(4.03\text{ GeV})^2$
$\lvert f(q^2)\rvert/\lvert f(0)\rvert$	0.034 ± 0.006	0.024 ± 0.006	0.0074 ± 0.0023

8 Acknowledgements

This research is supported by the U.S. Department of Energy research grant number DE-FG03-94ER40833. This work was aided by my colleagues in the Hawaii BES group and informative conversations with Eric Braaten.

References

[1] M.E.B. Franklin *et al.* (Mark II Collaboration), Phys. Rev. Lett. **51**, 963 (1983).

[2] J.Z. Bai *et al.* (BES Collaboration), Phys. Rev. **D54**, 1221 (1996); J.Z. Bai *et al.* (BES Collaboration), *Search for $\psi' \to$ Vector + Pseudoscalar Decays*, paper submitted to the 1995 International Symposium on Lepton and Photon Interactions at High Energies, Beijing, China.

[3] W-S. Hou, and A. Soni, Phys. Rev. Lett. **50**, 569 (1983); M. Anselimo *et al.* , Phys. Rev. **D50**, 595 (1994); W-S. Hou, Phys. Rev. **D55**, 6952 (1997).

[4] S.J. Brodsky, G.P. LePage, and S.F. Tuan, Phys. Rev. Lett. **59**, 59 (1987).

[5] M. Chaichian and N.A. Törnqvist, Nucl. Phys. **B323**, 75 (1989).

[6] S.S. Pinsky, Phys. Lett **B236**, 479 (1990);

[7] S.J. Brodsky and M. Karliner, Phys. Rev. **78**, 4682 (1997).

[8] Y-Q. Chen and E. Braaten, Phys. Rev. Lett. **80**, 5060 (1998).

[9] R.M. Barnett *et al.* (PDG), Phys. Rev. **D54**, 1 (1996).

[10] T. Appelquist and H.D. Politzer, Phys. Rev. Lett. **34**, 43 (1975); and A. De Rújula and S.L. Glashow, *ibid*, page 46.

[11] S.W. Ye *Analysis memo of $\psi(2S) \to \omega\pi^0$, $\omega\eta$*, June 1997.

[12] C.Z Yuan, BES analysis memo, March 1996.

[13] D. Coffman *et al.* (Mark III Collaboration), Phys. Rev. **D38**, 2695 (1988).

[14] J.Z. Bai *et al.* (BES Collaboration), *Branching fractions for ψ_{2S} decays to octet-baryon pairs*, paper submitted to the 1995 International Symposium on Lepton and Photon Interactions at High Energies, Beijing, China.

[15] Because some of the unseen K^*K modes have two neutral K mesons, it was not obvious that the use of $\mathcal{B}(K^{*0} \to K^+\pi^-) = 2/3$ was appropriate for this case. I thank Bill Dunwoodie for carefully verifying that, in fact, it is.

[16] To derive a 90% CL limit on the ratios $\mathcal{B}(\psi_{2S} \to K^{*0}\overline{K^0})/\mathcal{B}(\psi_{2S} \to K^{*+}K^-)$ and $R_{K^{*0}K}/R_{K^{*+}K^-}$, I reduced the measured value for the numerator by one sigma and divided by the experimental upper limit on the denominator.

[17] G. Bonneau and F. Martin, Nucl. Phys. **B27**, 380 (1971).

[18] A. Seiden, H.F-W. Sadrozinski, and H.E. Haber, Phys. Rev. **D38**, 824 (1988).